



# Characterization of soil-derived *Bacillus subtilis* metabolites against breast cancer: In vitro and in silico studies

Ayesha Irfan Hashmi<sup>1</sup> · Mehwish Iqtedar<sup>1</sup> · Hamid Saeed<sup>2</sup> · Nadeem Ahmed<sup>3</sup> · Roheena Abdullah<sup>1</sup> · Afshan Kaleem<sup>1</sup> · Muhammad Athar Abbasi<sup>4</sup>

Received: 8 January 2025 / Accepted: 6 March 2025 / Published online: 17 April 2025  
© The Author(s) 2025

## Abstract

Breast cancer remains one of the most challenging and widespread cancers among women globally that warrants further investigations for novel agents to minimize side effects and disease recurrence. In this study, a soil bacterium was isolated and 16S rRNA nucleotide sequence homology and resultant phylogenetic tree analysis confirmed *Bacillus subtilis* (CP020102.1). The crude extract of bacterial strain showed cytotoxicity (cell viability 63.1%) against human breast cancer cell line MCF-7 through MTT assay followed by further analysis through preparative HPLC showing 29 active fractions. Among all fractions, fraction 16 demonstrated cytotoxic potential as low as 54.03%. The spectral data of LC–MS, NMR and FTIR identified the bioactive compound as isatin based bacterial metabolite (Z)-N'-(1-hexyl-2-oxoindolin-3-ylidene)-4-methylbenzenesulfonohydrazide. This bioactive compound upon in silico docking analysis with HER2 showed a binding energy of -8.8 kcal/mol. ADMET calculations determined the pharmacokinetic behavior of the compound revealing acceptable distribution and absorption profiles. The drug-likeness of the compound was confirmed based on the Lipinski rule with zero violations. Molecular dynamic simulation (MDS) was also performed for 100 ns and a stable RMSF plot was observed. The results strongly propose that the identified compound has immense potential to be considered a drug candidate to develop further against human breast cancer.

**Keywords** *Bacillus subtilis* · Secondary metabolite · Anticancer activity · MCF-7 · Molecular docking

## Abbreviations

MTT	3-(4,5-Dimethylthiazol-2-yl)-2,5-diphenyltetrazolium bromide
HPLC	High Performance Liquid Chromatography
LC-MS	Liquid Chromatography-Mass Spectrometry
FTIR	Fourier Transform Infrared Spectroscopy
NMR	Nuclear Magnetic Resonance Spectroscopy
HER2	Human Epidermal Growth Factor Receptor 2

## 1 Introduction

Breast cancer remains the most prevalent type of cancer among women worldwide (Akbari et al. 2011; Houghton and Hankinson 2021), with its occurrence in 157 out of 185 countries (Arnold et al. 2022). The World Health Organization has reported 2.3 million new cases and 0.67 million mortalities globally in 2022, with almost half of all cases

✉ Mehwish Iqtedar  
miqtedar@gmail.com; mehwish.iqtedar@lcwu.edu.pk

✉ Hamid Saeed  
hamid.pharmacy@pu.edu.pk

Ayesha Irfan Hashmi  
iayasha240@gmail.com

Nadeem Ahmed  
Nadeem.cemb@pu.edu.pk

Roheena Abdullah  
roheena.abdullah@lcwu.edu.pk

Afshan Kaleem  
afshan.kaleem@lcwu.edu.pk

Muhammad Athar Abbasi  
abbasi@gcu.edu.pk

<sup>1</sup> Department of Biotechnology, Lahore College for Women University, Lahore, Pakistan

<sup>2</sup> University College of Pharmacy, University of the Punjab, Allama Iqbal Campus, Lahore 54000, Pakistan

<sup>3</sup> Centre of Excellence in Molecular Biology (CEMB), University of the Punjab, Lahore, Pakistan

<sup>4</sup> Department of Chemistry, Government College University, Lahore, Pakistan

occurring in women associated with no specific risk factors except gender and age. Breast cancer is considered a pressing health concern as it is the leading cause of death from cancer in women (Trayes and Cokenakes 2021; Zhang et al. 2024).

Numerous receptors are associated with the development of breast cancer. In about 30% of breast cancer tumors, Human epidermal growth factor receptor 2 (HER2) is overexpressed and is responsible for the aggressiveness of tumors resulting in lower survival chances (Mitri et al. 2012; Schettini et al. 2020). The most common mode of treatment for breast cancer is chemotherapy, which has the potential to cause both acute and chronic side effects, from short-term discomfort to long-term issues that may emerge years after the treatment is received (Partridge and Winer 2004; Faruk 2021). These undesired side-effects and toxicity caused to normal cells by conventional treatment options like radiotherapy, chemotherapy, targeted immunotherapy or even surgery, can be avoided by the use of natural compounds from natural sources that offer broad-spectrum benefits with minimal to no side effects (Caicedo et al. 2012; Franzoi et al. 2021).

It is reported that about 13,000 natural compounds, each possessing different therapeutic and pharmacological characteristics, have been isolated from bacterial sources (Mohan et al. 2022). The vast diversity of bioactive secondary metabolites produced by bacteria has been known and valued for over a century (Tyc et al. 2017). Many of these metabolites have been reported as anti-cancer agents against different types of human cancers (Kennedy et al. 2015; Ali et al. 2016; Osama et al. 2022). Some of the prominent bacterial derived anti-cancer compounds currently in clinical use are Bleomycin (Chen et al. 2020; Shaikh et al. 2023), Dactinomycin (Kyrgiou et al. 2006; Liu et al. 2019), Doxorubicin (Thorn et al. 2011; Zhang et al. 2021), Carfilzomib (Gay et al. 2021; Burke et al. 2022). Among such compounds Ixabepilone, a bacterial metabolite (Mohan et al. 2022), is being used in the treatment of breast cancer (Cristofanilli 2012; Li et al. 2017; Azizah et al. 2024).

Numerous effective anticancer agents, e.g. sunitinib and semaxanib, consist of an isatin scaffold, signifying that isatin is an active moiety for developing novel anticancer agents (Alanazi et al. 2023). Many secondary metabolites that contain isatin moiety are obtained from bacterial sources (Wu et al. 2015; Ayuningrum et al. 2019; Triningsih et al. 2023).

The genus *Bacillus* produces secondary metabolites with antiviral (Abdel-Nasser et al. 2024; Salazar et al. 2023), antibiotic (Tran et al. 2022; Caulier et al. 2019), anti-cancer (Aimaier et al. 2023; Shao et al. 2021) potential. *Bacillus subtilis* is commonly found in soil and has been known to produce bioactive compounds of various chemical nature, having linear or cyclic branching structures, which are

particularly significant for their anti-tumor potential (Kaspar et al. 2019; Dan et al. 2021). Different bioactive compounds have been sourced from *Bacillus subtilis* that showed cytotoxicity towards breast cancer cells and were subjected to molecular docking analysis with HER2 protein of breast cancer, demonstrating significant binding energies (Kumari and Ram 2021).

This study aimed to identify the anticancer potential and structure of bioactive secondary metabolites extracted and purified from the culture medium of *Bacillus subtilis* by in vitro and in silico computational analysis.

## 2 Materials and methods

### 2.1 Sample collection and isolation of bacteria

A total of 30 soil samples were collected from various locations in Lahore, Pakistan, focusing on the upper soil layer where bacterial colonies are most abundant (Mishra 2013). Roughly 10 g of soil from each site was collected with the help of a sterile spatula and containers. Soil suspensions were prepared by mixing 1 g of each soil sample 10 mL of distilled water. Furthermore, by employing tenfold serial dilution, 1 mL of the suspension was diluted in 9 mL of distilled water stepwise up to  $10^{-6}$ . (Kannan et al. 2018). The medium used in this research was nutrient agar (5.0 g/L peptone, 5.0 g/L NaCl, 1.5 g/L beef extract, 1.5 g/L yeast extract, 15 g/L agar) (Abdulkadir and Waliyu 2012). Initially, the spread plate method was employed in which 100  $\mu$ L from each dilution was spread onto nutrient agar plates with the help of a sterile glass spreader. Plates were incubated at 37 °C until bacterial colonies appeared. Pure bacterial cultures were obtained by the streak plate method and incubated at 37 °C (Uddin and Chowdhury 2022).

### 2.2 Inoculum development and production of secondary metabolites

The inoculum was prepared according to the protocol described by (Thomas et al. 2011). Single and distinct colony from each bacterial pure culture was inoculated into 5 mL of Nutrient Broth (5.0 g/L peptone, 5.0 g/L NaCl, 1.5 g/L beef extract, 1.5 g/L yeast extract) having pH  $7.0 \pm 0.2$  and incubated in shaking incubator at 120 rpm and 37 °C for 24 h. Upon reaching adequate turbidity, indicating bacterial growth, the inocula were scaled up by transferring them into 20 mL of fresh medium. This production medium was incubated under identical conditions as previously described for 96 h. After it reached its maximal growth ( $OD_{600}$ : 2.5) (Numan et al. 2022), differential centrifugation was employed in which the culture

broth was centrifuged for 15 min at 3000 rpm (1,006  $\times g$ ) using a low-speed bench top centrifuge with the rotor radius of 10 cm at room temperature ( $\sim 25^\circ\text{C}$ ) to obtain clear supernatant.

### 2.3 Extraction of secondary metabolites

The extraction of metabolites was carried out by the liquid–liquid extraction method, as described by (Burianek and Yousef 2000). In this method, equal amounts of supernatant and a freshly prepared mixture of chloroform–methanol (2:1 v/v) were vortexed in a sterile Eppendorf and centrifuged at 16,100  $g$  for 5 min at  $4^\circ\text{C}$  to separate the phases. The separated polar phase (upper layer) was transferred to a new sterile falcon without disturbing the rest of the content. The extracts were concentrated using rotary vacuum evaporator under reduced pressure. In the next step, the concentrated extracts were dried at  $60^\circ\text{C}$  in a hot air oven. The final dried crude extract was stored at  $-20^\circ\text{C}$  until further use.

### 2.4 Primary screening for cytotoxic activity

The cytotoxic potential of the bacterial extracts was evaluated using the MTT (3-(4,5-Dimethylthiazol-2-yl)-2,5-Diphenyltetrazolium Bromide) assay (Mosmann 1983) against the MCF-7 human breast cancer cell line. Cells were seeded at a density of  $1 \times 10^4$  cells per well in a flat bottom 96-wellplate, with the cell culture media consisting of 88% Dulbecco's Modified Eagle's Medium (DMEM), 10% Fetal Bovine Serum (FBS), and 2% Penicillin–Streptomycin (Penstrep) per 100 mL of total medium. The cells were incubated at  $37^\circ\text{C}$  in a humidified 5%  $\text{CO}_2$  incubator for 24 h. After the incubation period, the culture medium was replaced, and cancer cells were treated with 20  $\mu\text{L}$  bacterial extracts (100  $\mu\text{g}/\text{mL}$  dissolved in DMSO) for an additional 24 h at  $37^\circ\text{C}$ . Following treatment, 10  $\mu\text{L}$  of MTT solution (5  $\text{mg}/\text{mL}$ ) was added to each well, and the plate was incubated for another 4 h at  $37^\circ\text{C}$ . After incubation, the medium was carefully removed, and the resulting formazan crystals were solubilized in 50  $\mu\text{L}$  of DMSO per well. Absorbance was measured at 570 nm using an ELISA plate reader to determine cytotoxicity (Akbarizare et al. 2020). The results were expressed as a percentage of viable cells compared to controls. Cell viability was calculated using the following formula (Sebola et al. 2020).

$$\% \text{ Cell viability} = \frac{(E_a - B_a)}{(C_a - B_a)} \times 100,$$

where  $E_a$  is the absorbance of the extract,  $B_a$  is the absorbance of the blank, and  $C_a$  is the absorbance of the control.

### 2.5 HPLC fractionation

Crude extracts exhibiting the highest anticancer activities were subjected to preparative High-Performance Liquid Chromatography (HPLC) for fractionation and were collected based on their retention times (RT) (Rajivgandhi et al. 2018). The analysis was performed with Agilent Technologies 1260 Infinity II HPLC system equipped with a Diode Array Detector (DAD). A C-8 column (5  $\mu\text{m}$ , 250  $\text{mm} \times 4 \text{ mm}$ ) was used with methanol as the mobile phase. The injection volume was set to 20.0  $\mu\text{L}$ , with a flow rate of 1.0  $\text{mL}/\text{min}$ . The column temperature was maintained at  $40^\circ\text{C}$ , and detection was carried out at a wavelength of 210 nm. All the fractions were collected in sterile falcons, lyophilized, and stored at  $-20^\circ\text{C}$  until further use. The retrieved purified fractions were further subjected to secondary screening (30  $\mu\text{g}/\text{mL}$ ) for their cytotoxic effect against MCF-7 cell lines.

### 2.6 Spectral studies and structure elucidation

$^1\text{H}$ NMR (nuclear magnetic resonance) spectra of bioactive secondary metabolite was recorded at 300 MHz and  $^{13}\text{C}$  NMR at 75 MHz on (Bruker Model: Avance-II) spectrophotometer. All chemical shifts are expressed in ppm.  $\text{CDCl}_3$  was used as the solvent for NMR spectroscopy (Raghava Rao et al. 2017).

Fourier transform infrared (FTIR) spectrum of bioactive secondary metabolite was obtained using an FTIR spectrometer (model NICOLET 6700; Thermo-scientific). The spectra covered the infrared region  $4000\text{--}500 \text{ cm}^{-1}$ .

LC–MS analysis was performed using Agilent 6300 ion trap LC/MS systems. Chromatographic separation was achieved with an isocratic mode with acetonitrile (ACN) as the mobile phase at a flow rate of 0.5  $\text{mL}/\text{min}$ . MS detection was carried out using electrospray ionization (ESI). The mass scanning range was up to 1000  $m/z$  and mass detection was performed in the negative ion mode. Chemstation software was used for data processing. Thin-layer chromatography (TLC) was performed using Merck silica gel 60F254 pre-coated aluminum plates with  $n$ -hexane ethyl acetate (4:6) as the mobile phase. UV-active compounds were visualized under UV light at 254 and 365 nm, while different staining agents were applied for UV-inactive compounds.

### 2.7 Molecular characterization

The bacterial isolate was identified through 16S rDNA sequencing by using universal primer pairs (Ashfaq et al.

2021). Sequencing primers 785F (5'-GGA TTA GAT ACC CTG GTA-3') and 907R (5'-CCG TCA ATT CMT TTR AGT TT-3') were used for the sequencing process. PCR amplification was performed using primers 27F (5'-AGA GTT TGA TCM TGG CTC AG-3') and 1492R (5'-TAC GGY TAC CTT GTT ACG ACT T-3'). The phylogenetic relationship of the isolate was determined based on sequence homology using the Neighbor-Joining method (White et al. 1990; Bellemain et al. 2010).

## 2.8 In silico studies

Various in silico studies, including 3D structure development, prediction of pharmacokinetics and drug likeness, molecular docking and molecular dynamic simulation studies were performed for the validation of selected bioactive metabolite and its interactional behavior towards breast cancer receptors.

### 2.8.1 Structure determination of bioactive metabolite

The general molecular and formula based parent structure of the selected compound determined through NMR was further used to generate its canonical SMILES by using the online tool Cheminfo (<https://www.cheminfo.org/flavor/malaria/Utilities/SMILESgeneratorchecker/index.html>).

The generated SMILES was further used to draw the 2D structure in SDF file format through Chemdraw, an online chemistry server (<https://revvitysignals.com/products/research/chemdraw>) (Cousins 2011).

0.3D representation in the ball and stick model was determined by the Pymol (<http://www.pymol.org/pymol>) software and saved in PDB file format (Schrödinger and DeLano 2020). This PDB file format of the compound was used as ligand compound for further studies.

### 2.8.2 Prediction of pharmacokinetics and druglike properties

Druglike properties of the selected compound were predicted by an online tool SWISSADME (<http://www.swissadme.ch/>) (Daina et al. 2017).

### 2.8.3 Selection and retrieval of oncogenic receptor proteins

Different breast cancer receptor proteins such as Estrogen Receptor Alpha (ER $\alpha$ ), Human Epidermal Growth Factor Receptor 2 (HER2), Progesterone Receptor (PR), VEGFR2 (Vascular Endothelial Growth Factor) and Polo-like Kinase (PLK1) were selected based on their potential role in disease and occurrence of progression (Gam 2012).

3 dimensional crystallized structures of the all-mentioned proteins were downloaded from RCSB PDB database (<https://www.rcsb.org/>), having unique PDB ID (ER $\alpha$ -1ERE, HER2-3PP0, PR-1A28, VEGFR2-2VPP, PLK1-3D5U) (Burley et al. 2021). All these receptor proteins were used as target proteins against above mentioned bioactive metabolite.

### 2.8.4 Preparation of target proteins and ligand compound

Discovery Studio tool (<https://discover.3ds.com/discovery-studio-visualizer-download>) was used to prepare target proteins by removing all the attached water molecules, ligands, metals and ions by San-Diego (2021). PyMol viewer software was employed to view and save prepared targets in PDB file formats. Ligand (bioactive metabolite) was also saved in the same PDB file format and was used for molecular docking analysis with target proteins.

### 2.8.5 Molecular docking analysis

All the PDB files of target proteins were converted to PDBQT files to run docking by Autodock Vina software of MGL tools version 1.5.7 (Trott and Olson 2010). Hydrogen molecules and kollmann charges were added for the energy refinement and these refined PDB structures were converted to PDBQT files by Vina software. The ligand (bioactive compound) was also prepared by adding torsion angles and the torsion root was adjusted. Various commands were made from the command prompt to run the docking experiments for each target. The grid dimension was adjusted at 1.000 Å spacing and numbers of points of all three dimensions were set as 100. The grid values for X, Y, and Z coordinates were 21.407, 31.289 and 14.676, respectively. PyMOL viewer software and Discovery Studio tool (<https://discover.3ds.com/discovery-studio-visualizer-download>) were used to analyze the docking results. Top receptors protein was selected and used for simulation studies, selection was made on binding energy and residual interactions.

### 2.8.6 Molecular dynamic simulation analysis

The best docked complex (HER2) was evaluated further by molecular dynamic simulation studies to check the interactional behavior of the docked complex in physiological conditions (Huang et al. 2023). Desmond Software, LLC v3.6 module, version 2019, was used to perform MD simulation analysis, which was carried out for 100 ns. Wizard in Maestro tool was employed for the preparation of target proteins constant temperature of 300 K and 1 atm pressure with OPLS-2005 all atoms force field. 0.12 M NaCl ions were added to maintain the ionic concentration at neutral charges. Following a successful



100 ns simulation, the results were analyzed, and the two most common metrics, root mean square deviation (RMSD), root mean square fluctuations (RMSF), were used to evaluate the stability of protein–ligand docked complexes (Ayan et al. 2017).

## 2.9 Statistical analysis

All the experiments were performed in triplicate. One-way ANOVA was used to test the significant ( $p \leq 0.05$ ) differences between means of experimental values by using SPSS program version 16.

## 3 Results and discussion

### 3.1 Bacterial isolates

Out of 30 soil samples, 200 bacterial isolates were obtained. Soil samples proved very effective sources of bacteria that

have the potential to produce cytotoxic metabolites of a diverse chemical nature (Tyc et al. 2017; Gislin et al. 2018). Bacterial genera like *Bacillus* (Aimaier et al. 2023; Shao et al. 2021; Shalini et al. 2024), *Streptomyces* (Hamed et al. 2024; Sethi et al. 2024; Nascimento Chaves et al. 2024), *Salmonella* (Aganja et al. 2022; Kalia et al. 2022), *Escherichia* (McCoy et al. 2021; Nakkarach et al. 2021), *Pseudomonas* (Sereena and Sebastian 2020; Subbiah et al. 2024), and *Clostridium* (Yaghoubi et al. 2022; Liu et al. 2023) have been reported to produce anticancer metabolites.

### 3.2 Extraction of secondary metabolites

The usage of a chloroform-containing solvent system for the extraction of bacterial secondary metabolites is supported by various previous studies (Burianek and Yousef 2000; Anantha et al. 2016; Abdelaziz et al. 2022) in which it was verified that the chloroform based organic solvent system may improve the extraction of bacterial compounds by many folds.

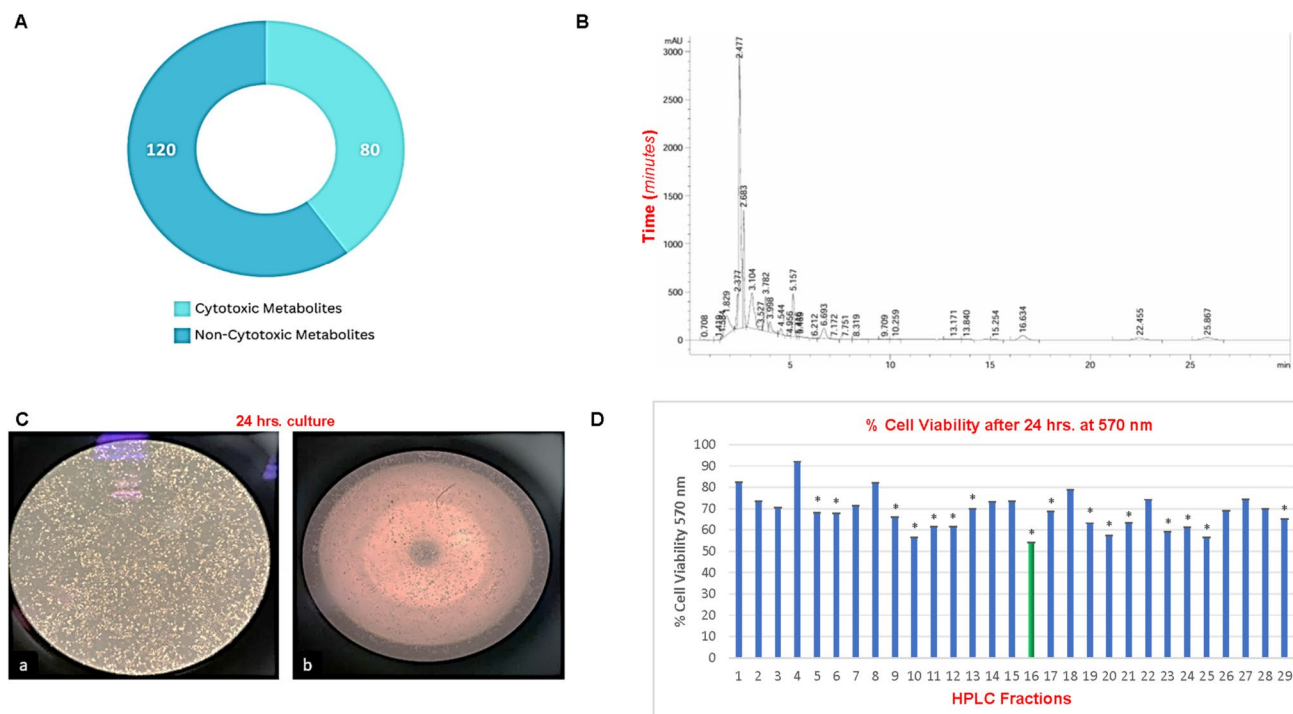


**Fig. 1** **A** Distribution of cytotoxic and non-cytotoxic metabolites following primary screening against MCF-7 cells. **B** HPLC chromatogram of the crude cytotoxic extract 74 following primary screening. The chromatogram shows 29 distinct peaks between 0 to 26 min at 210 nm. **C** Percentage cell viability (%) at 570 nm for each HPLC

fraction. Fraction 16 (green bar) exhibited a mean absorbance of 0.41, corresponding to 54.03% viability. Data were analyzed by one-way ANOVA ( $p \leq 0.05$ ). Asterisks (\*) indicate statistically significant differences from the control. **D** Breast cancer cells before and after 24-h treatment with fraction 16

### 3.3 Primary screening for cytotoxic activity

Out of 200 bacterial extracts, 80 were cytotoxic against MCF-7 cells (Fig. 1A). Three extracts, 76, 27, and 74, showed cell viability values of 64.8%, 63.7% and 63.1%, respectively. It has been confirmed in recent studies that bacterial metabolites exhibit cytotoxic properties against different types of cancers (Laliani et al. 2020; Behzadi et al. 2021; Elmanama et al. 2020).

### 3.4 HPLC fractionation

The crude extract demonstrating the highest cytotoxic activity (extract 74) in primary screening, was subjected to fractionation using preparative HPLC resulting in the identification of **29 distinct fractions**, each corresponding to a unique peak in the chromatogram obtained at 210 nm with retention times ranging from 0.708 to 25.867 min (Fig. 1B). Notably, Peak 6 (tR: 2.477 min) exhibited the highest percentage area (38.74%), suggesting it is the most abundant component in the extract. Other significant peaks include Peak 7 (tR: 2.683 min) and Peak 8 (tR: 3.104 min), with percentage areas of 11.43% and 12.00%, respectively. These fractions are expected to contain the bioactive compounds that were responsible for cytotoxicity induction during primary screening. These fractions were further subjected to secondary screening.

Previous research has shown that HPLC fractionation is a well-established method for isolating bioactive compounds from complex extracts of both bacteria and plants. For instance, the crude extract of *Bacillus sp.* strain B29 produced 17 fractions (Sihem et al. 2011), and the extracts of *Glycyrrhiza glabra* produced 20 fractions (Rahman et al. 2018). Chalasani et al. (2015) and Shalini et al. (2024) performed RP-HPLC on *Bacillus subtilis* and *Bacillus cereus* extracts, respectively, and obtained various peaks between the retention time of 5 to 30 min.

### 3.5 Secondary screening for cytotoxic activity

Among all the fractions tested, fraction 16 (30 µg/ml in DMSO) showed the lowest cell viability of 54.03%, indicating it had the most significant cytotoxic effect (Fig. 1C). This suggests that Fraction 16 contains potent bioactive compounds that significantly reduce cell viability (Fig. 1D), making it the most promising candidate for further investigation. The cytotoxic activity of a bioactive compound increases when used in a purified form. For instance, in another study, a bioactive metabolite extracted from culture supernatant of *B. vallismortis* BIT-33 was purified by Jeong et al. (2008), and the compound showed direct cytotoxic and apoptotic effects on colon cancer cells.

Other fractions, such as Fraction 25 (56.38% cell viability) and Fraction 9 (65.89% cell viability), exhibited notable cytotoxic effects but were less effective than Fraction 16. The observed decrease in cell viability confirms that these fractions have substantial cytotoxic potential and warrant additional study to elucidate their active components and predictions of their drug-likeness abilities.

### 3.6 Identification of isolate 74 using 16S rRNA profile

Isolate 74 was selected and identified as *Bacillus subtilis* with 99% similarity and then deposited at GenBank with accession number CP020102.1. Figure 2A shows the phylogenetic tree of *Bacillus subtilis* CP020102.1

### 3.7 LCMS data of compound

The LC–MS analysis of the bioactive compound from Fraction 16 and the protonated molecular ion peak  $[M + H]^+$  was observed at  $m/z$  400.12 (Fig. 2B), indicating that the compound's molecular weight is 399.12 amu. Fragmentation peaks were also observed at  $m/z$  365.8 and  $m/z$  507.5, likely representing the loss of smaller functional groups or possible adducts with solvent molecules. The fragment at  $m/z$  365.8 corresponds to a neutral loss of approximately 34 amu, potentially from side-chain cleavage. The peak at  $m/z$  507.5 may indicate the presence of adducts, possibly due to interaction with matrix ions or solvent components.

The molecular weight of 399 Da excludes the possibility of metabolites being iturins, fengycins, and surfactins known as *Bacillus* lipopeptides and have molecular weight between 1,000–1,200 Da (Ongena and Jacques 2008). Also, it is unlikely to be a part of the class II or III bacteriocins because the latter include larger peptides and protein complexes, many of which have molecular weights over several thousand Da (Wang et al. 2024). Due to its lower molecular weight and anticancer activity, this compound may contain an aromatic ring, similar to other biologically active bacterial metabolites, including phenazines and polyketides, which contain aromatic rings and are target specific and bioavailable (Pereira et al. 2009; Laursen and Nielsen 2004).

### 3.8 FTIR spectroscopy analysis

The FTIR spectrum (Fig. 2C) of the bioactive compound from Fraction 16 provides detailed insights into its molecular structure. Signals at specific frequencies suggest the presence of various functional groups:  $3175\text{ cm}^{-1}$  indicates N–H stretching vibrations of secondary amides, and  $2959\text{ cm}^{-1}$  corresponds to Csp<sup>2</sup>–H stretching, which is characteristic of aromatic rings. Peaks at  $2935$  and  $2869\text{ cm}^{-1}$  indicate asymmetric and symmetric stretching vibrations,

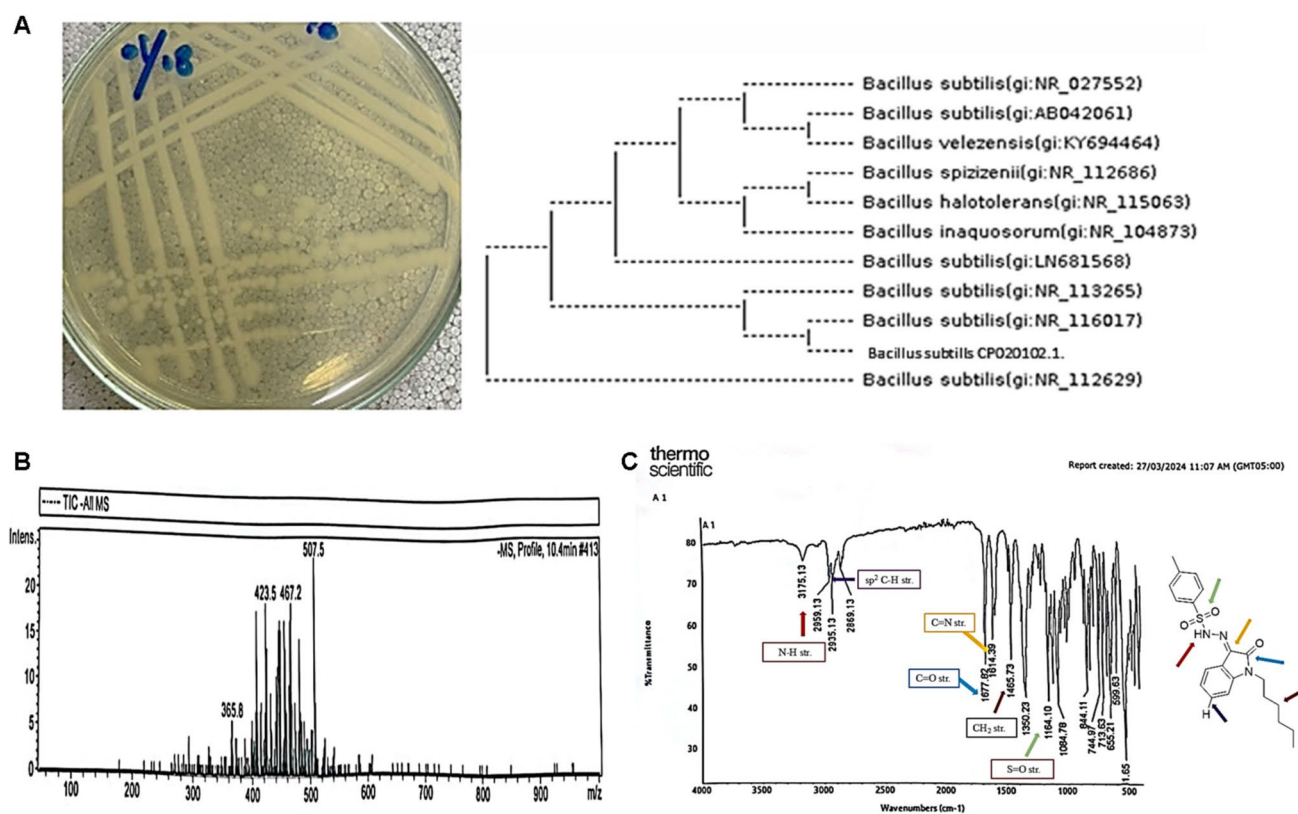


**Fig. 2** **A** Phylogenetic tree of *Bacillus subtilis* CP020102.1. **B** LC-MS Spectrum of Bioactive Compound from Fraction 16. **C** FTIR spectrum of the bioactive compound from Fraction 16, highlighting

ing key functional groups including amides, aromatic rings, methyl groups, and sulfone linkages

respectively, of a  $sp^3$  hybridized methyl group. Weak absorptions between 2000 and 1677  $cm^{-1}$  suggest overtone and combination bands that help determine ring substitution patterns. A strong absorption at 1667  $cm^{-1}$  is attributed to the carbonyl stretching of an amide or cyclic amide. Additional signals at 1614, 1601, and 1465  $cm^{-1}$  correspond to C=N and C=C stretching and  $Csp^3-H$  bending, with the peak at 1465  $cm^{-1}$  indicating the presence of a methylene group. Absorptions at 1350 and 1164  $cm^{-1}$  indicate S=O group stretches, and bands at 1233 and 1033  $cm^{-1}$  suggest a phenyl alkyl ether linkage. Signals at 714  $cm^{-1}$ , 844  $cm^{-1}$ , 713  $cm^{-1}$ , and 655  $cm^{-1}$  provide further insights into  $CH_2$  bending and aromatic substitution patterns. The FTIR spectrum confirms the presence of amide, aromatic ring, ether linkage, and aliphatic methylene functionalities in the bioactive compound of Fraction 16.

Several anticancer *Bacillus* derived metabolites are reported that are heterocyclic and contain sulfur and nitrogen (Zhang et al. 2022), for instance, Bacillamide A is produced by *Bacillus* sp. SY-1 (Jeong et al. 2003), Bacillamide B and C are produced by *Bacillus endophyticus* (Socha et al. 2007) and Bacillamide F is produced by *Bacillus atrophaeus* (Zhang et al. 2022). Furthermore, the presence of nitrogen

and sulfur in a heterocyclic compound studied for multi-target pharmacology, especially in cytotoxic applications, may increase therapeutic efficiency in cancer (Carradori et al. 2022; Drakontaeidi et al. 2024).

### 3.9 $^1H$ NMR analysis

In the  $^1H$  NMR spectrum of the bioactive compound from Fraction 16 (Fig. 3A), the appearance of a signal in the most de-shielded region at 12.60 ppm with the integration of one proton gave the evidence that one hydrogen attached with most de-shielded species such as aldehyde or amide ( $-NH-C=O$ ). The triplet with the integration of two protons at 3.69 ppm due to the two neighboring protons and high chemical shift indicated  $-CH_2$  group is further attached with heteroatom as ( $O-CH_2$  or  $N-CH_2$ ). The singlet having integration of three protons at 2.43 ppm indicates the proton of methyl with no neighboring proton attached with  $sp^2$  hybridized carbon. The multiplet ranging from 1.70–1.63 ppm with the integral of two protons indicates the presence of neighboring protons of different environments in the sample as ( $NH-CH_2-CH_2-CH_2$ ). The multiplet in the aliphatic region with the integral of six protons at 1.37–1.28 ppm

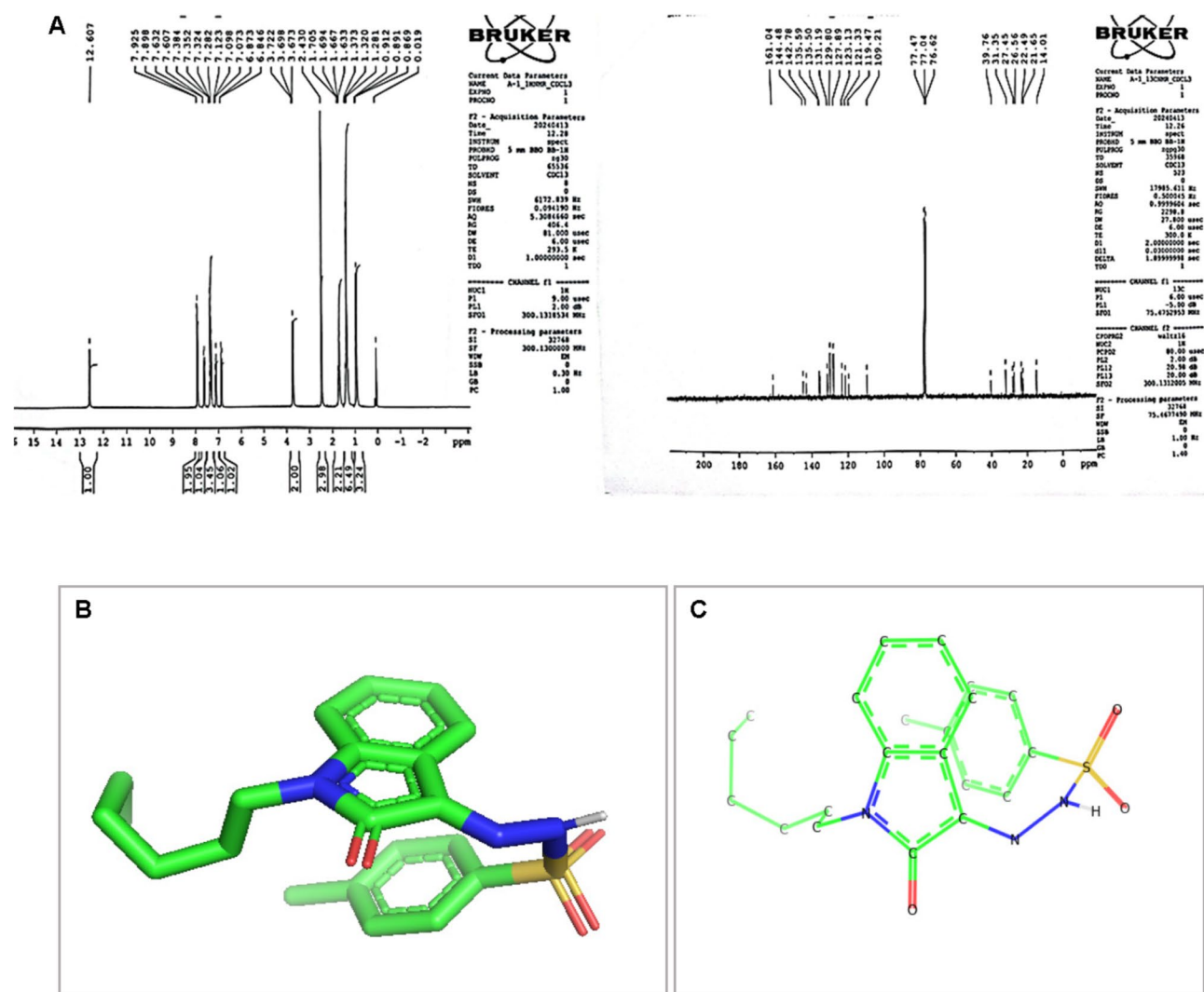


**Fig. 3** **A**  $^1\text{H}$ NMR and  $^{13}\text{C}$  NMR spectrum of the bioactive compound from Fraction 16. **B** 3D structure representation of bioactive compound. **C** 2D Structure representation of compound with molecular symbol

gave evidence of the presence of a long aliphatic chain as  $(\text{CH}_2\text{-CH}_2\text{-CH}_2\text{-CH}_2\text{-CH}_2)$ . The signals of eight aromatic protons appeared in the range of 7.92 to 6.84 ppm indicating the presence of two substituted benzene rings.

### 3.10 $^{13}\text{C}$ NMR analysis

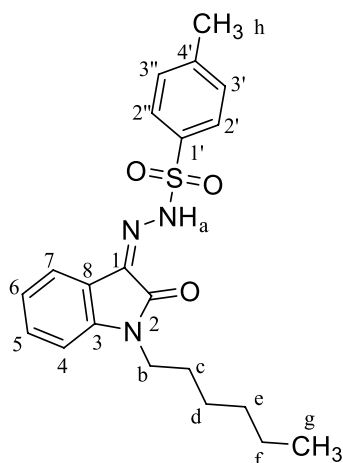
The  $^{13}\text{C}$  NMR of the bioactive compound from Fraction 16 demonstrated the most de-shielded signal at 161.0 indicating the presence of any carbonyl. The appearance of a signal at 135.5 ppm for carbon indicates the imine linkage ( $\text{C}=\text{N}$ ), it may also indicate the formation of imine linkage. The signal appeared at 39.7 ppm indicating the carbon directly attached to heteroatom i.e., N, O, S etc. The signals at 31.3, 27.4, 26.5, 22.4, 21.6 ppm and 14.0 ppm

showed the presence of long aliphatic chain of carbons, respectively. The signals of aromatic carbons are in the range of 144.4 to 109.2 ppm. Overall, from the  $^{13}\text{C}$  NMR results it was confirmed that seven carbons present in the aliphatic region, one signal of carbon carbonyl, and signals of eleven carbon in the aromatic region in structure of unknown compound.

NMR results shows that the structure contains isatin moiety. Isatin is reported to be isolated from natural sources including plants (Speranza et al. 2020; Marcelo et al. 2019) and microorganisms (Gil-Turnes et al. 1989) specifically bacteria (Shaaban et al. 2016; Grafe and Radics 1986).

### Spectral and physical characterization of bioactive compound





Appearance: Yellow solid; Melting Point: 220–225 °C; Rf: 0.47 (n-hexane: ethyl acetate, 6:4); FT-IR  $\bar{\nu}$  (cm<sup>-1</sup>): 3175 (N–H stretch of amide), 2959 (Csp<sup>2</sup>–H), 2935, 2869 (Csp<sup>3</sup>–H), 1677 (lactam C=O), 1614 (imine C=N), 1465 (–CH<sub>2</sub>– bending); <sup>1</sup>H NMR (300 MHz, CDCl<sub>3</sub>-d):  $\delta$  (ppm): 12.60 (1H, s, NH-a), 7.91 (2H, d, H-2', 2''), 7.61 (1H, d, H-7'), 7.38–7.28 (3H, m, H-3', 3'', 4), 7.09 (1H, t, H-6), 6.85 (1H, d, H-5), 3.72–0.86 (13H, H-b,c,d,e,f,g) aliphatic protons; <sup>13</sup>C NMR (75 MHz, CDCl<sub>3</sub>):  $\delta$  (ppm): 161.0 (C-2), 131.1 (C-3'), 144.4, 142.7, 135.5, 129.8, 127.8, 123.1, 121.3, 119.4, 109.2 (aromatic carbons); EI-MS (m/z): 507.5[M–107]–, 467.2, 423.5, 365.8;

### 3.11 In silico analysis

#### 3.11.1 3D Structure determination of compound for

The structure of bioactive compound was determined and PDB file was generated by computational tools. Figure 3B and C shows the 2D and 3D PDB structure of bioactive compound prepared for docking analysis.

#### 3.11.2 Prediction of pharmacokinetics

The bioactive compound was analyzed for pharmacokinetics properties by Swiss ADME tool and mainly checked for Lipinski rule of 5 along with drug likeness properties.

Results shows that bioactive compound fulfilled Lipinski rule of 5 and possess pharmacokinetics properties as well. According to this rule, a drug-like compound should have a molecular weight (MW) less than 500 g/mol, a log P less than 5, hydrogen bond donors less than 5, hydrogen bond acceptor less than 10 and rotatable bonds less than 10 (En-Nahli et al. 2023). Pharmacokinetics includes GI absorption and Blood Brain Barrier (BBB). Conclusively, it was found that the compound has drug-like properties and most of the predicted values lie within acceptable range (Table 1). Likewise, a study was reported where Swiss ADME tool was used to predict these properties and compound passed Lipinski rule of 5 along with other pharmacokinetics parameters were predicted to have drug like activity (Agour et al. 2022). Radar chart was also retrieved which shows that all drug properties all required physiochemical properties (lipophilicity, size, polarity, insolubility, instauration and flexibility) lies within the stability zone. Radar points with red line of the properties lie within optimal zone. The optimal zone shown by pink region (Fig. 4A). This is in reference with a study in which after fulfilling these six parameters within the pink region the compound was considered drug-like compound (Ritchie et al. 2011).

#### 3.11.3 Docking analysis

Molecular docking results revealed that the compound showed good binding score with Human Epidermal Growth Factor Receptor 2 (HER2) i.e. –8.8 kcal/mol and various residues shows interactions towards HER2. The larger the negative value of binding energy, the stronger the affinity of the ligand with the receptor (Shamsee et al. 2019). A study has been documented that the docked complex with least binding energy considered as the most potential docking pose (Terefe and Ghosh 2022).

Moreover, docking results revealed that Thr862 amino acid residue made hydrogen bond with 3.25 Å bond length represented by blue dashed line with target. Hence HER2 selected as top receptor target and used for further simulation studies. Docking interaction with high binding energy shows that compound may be predicted as anticancer compound against breast cancer (Fig. 4A, C and Table 2). Here the interaction with Thr amino acid was found significant also evident by a previous report regarding inhibitors

**Table 1** Pharmacokinetics examination and Lipinski rule of 5 predictions

Physicochemical properties		Pharmacokinetics		Drug likeness	
M.F	C <sub>21</sub> H <sub>25</sub> N <sub>3</sub> O <sub>3</sub> S	GI absorption	High	LipinskiRule of 5	Fulfill
M.W	399.51 g/mol				
HA	28	BBB permeant	Low	Lipinski violations	0 violations
HBA	4				
HBD	1				

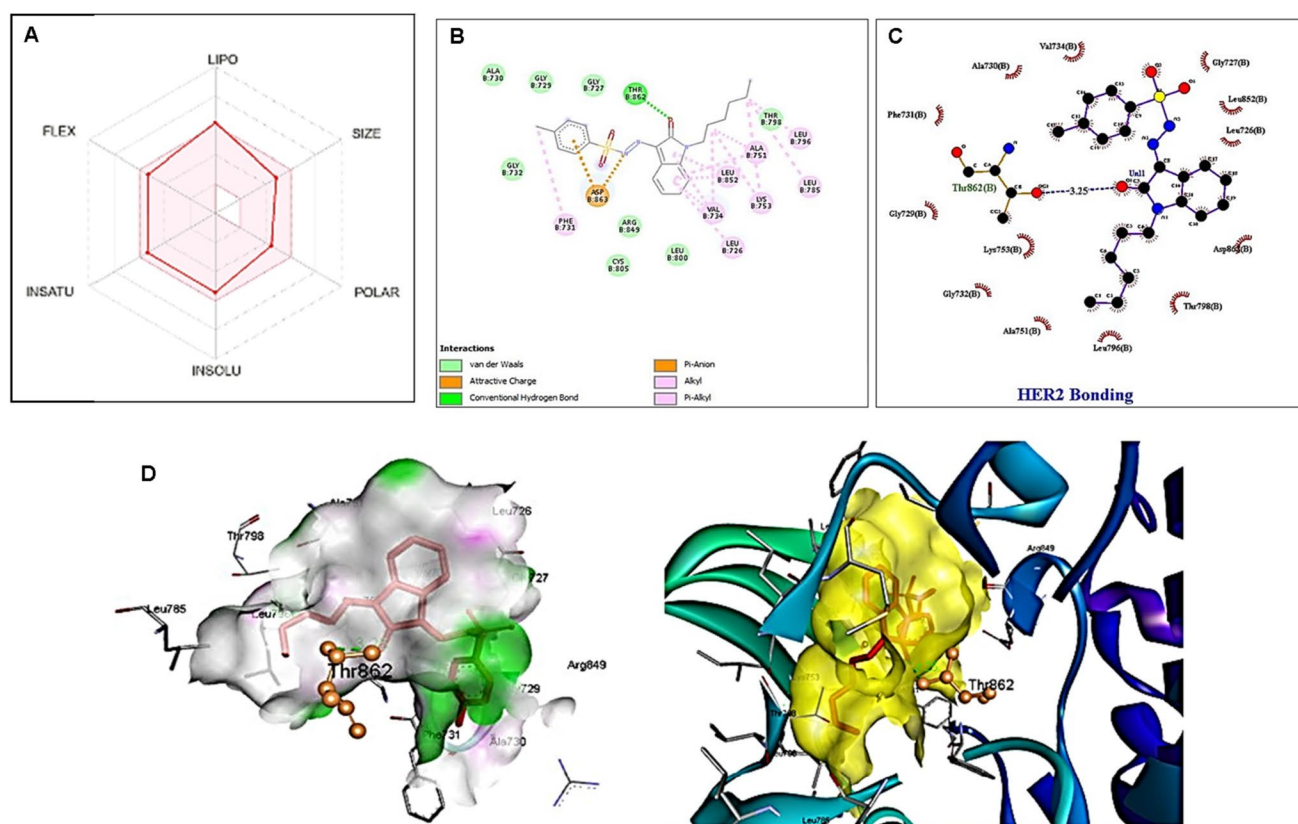


**Fig. 4** **A** RADAR chart determination of the compound. **B** 2D interaction of docking analysis between ligand compound and Target protein HER2: Discovery studio image representation of docking results.

**C** Ligplot image showing hydrogen bonding and hydrophobic interaction between compound and HER2. **D** 3D model of docked ligand with target protein

**Table 2** All the binding Score of docking complexes between bioactive compounds and target cancer receptor proteins

Sr. no	TARGET PROTEIN	BINDING ENERGY (Kcal/mol)	INTERACTING RESIDUES	RMSD
1	Estrogen Receptor Alpha (ER $\alpha$ )	-8.4	Glu380, Val534, Pro535, Met528, Leu384, Lys531, Thr347, Met522, Leu536, Trp383, Ala350, Leu346, Leu525, Asp351, Leu354	0.000
2	<b>Human Epidermal Growth Factor Receptor 2 (HER2)</b>	<b>-8.8</b>	<b>Ala730, Gly729, Gly727, Thr862, Thr798, Leu796, Ala751, Leu852, Leu785, Lys753, Val734, Leu726, Leu800, Arg849, Cys805, Phe731, Gly732</b>	<b>0.000</b>
3	Progesterone Receptor (PR)	-8.6	His770, Trp765, Met692, Gly762, Phe818, Lys822, Val729, Trp732, Met759, Leu758, Arg766, Glu695, Gln725, Pro696, Ser728, Ile699, Gln815, Val698, Asp697	0.000
4	VEGFR2(Vascular Endothelial Growth Factor)	-8.5	Lys868, Asp814, Arg1027, Ile1025, His1026, Ile888, Ile892, Asp1046, Leu889, Glu885, Ile1044, Cys1045, Val898, Leu1019, Val899, Val916, Val848, Leu1035, Phe1047	0.000

development against HER2 and their findings shows that Asn850, Leu852, Thr862, Asp863, and Phe864 of HER2 catalytic site are the important interacting amino acid (AA) residues with their selected (Sait et al. 2020). 3D model of selected docked complex was also generated (Fig. 4D).

### 3.11.4 Molecular stability evaluation of docked complex between bioactive compound and HER2 receptor protein

MD simulation results showed the estimation of RMSD value on y-axis with respect to time in 100 ns on X-axis for C $\alpha$  particles. Blue colored line represents the protein while

the pink colored lines represent RMSD evolution of the ligand. RMSD plots shows that complex gets stabilizes after 20 ns and little variations occurred after 35 ns and become unstable for 5 to 7 s only, equilibrates and stabilized till end. (Fig. 5A). Average RMSD values of the plot is 3.4 Å, which is quite acceptable. This is in agreement with a published study where a range of average RMSD values has been given and above-mentioned results falls in that range which shows that ligand fit to protein and remain stable at the binding site of the protein during the simulation (Riaz et al. 2024).

Root mean square fluctuations (RMSF) plot was also determined for simulation evaluation between target protein and ligand. This plot is used to analyze the residue wise fluctuations of the protein bounded with the ligand compound. Results shows that less fluctuations were observed during simulation and low RMSF values of both ligand and protein indicates that over all protein–ligand complex is stable (Fig. 5B and C). Most of the peaks are at lower level and green colored bars within the plot represent those residues which are in contact with ligand. Both the ligand and protein RMSF average values are 3.0 Å and 3.1 Å respectively

and these values shows that complex used for simulation is highly stable as lower the value the more stability is present. A study has been published in which a docked complex of HER2 with a screened molecule represent and amino acids fluctuations found between RMSF:  $\sim 4.0$ – $6.5$  Å during the simulation process of 100 ns and their collectively results showed the stability of docking in the defined active site of HER2 (Balogun et al. 2022).

Most important simulation examination is protein ligand contacts which is also monitored during molecular dynamic simulation of HER2 with the bioactive compound to evaluate its stability. This graph shows how many and which type of bonding is present between ligand and target complex used for simulation studies. HER2 results revealed that almost 5 hydrogen bonds, various hydrophobic and ionic interactions present with ligand and target (Fig. 5D). Green bars represented that 5 hydrogen bonds are present which shows strong stable interaction. In accordance with in silico research where lead compound was identified computationally from *Enterococcus faecium* strains, it has been concluded that hydrogen and

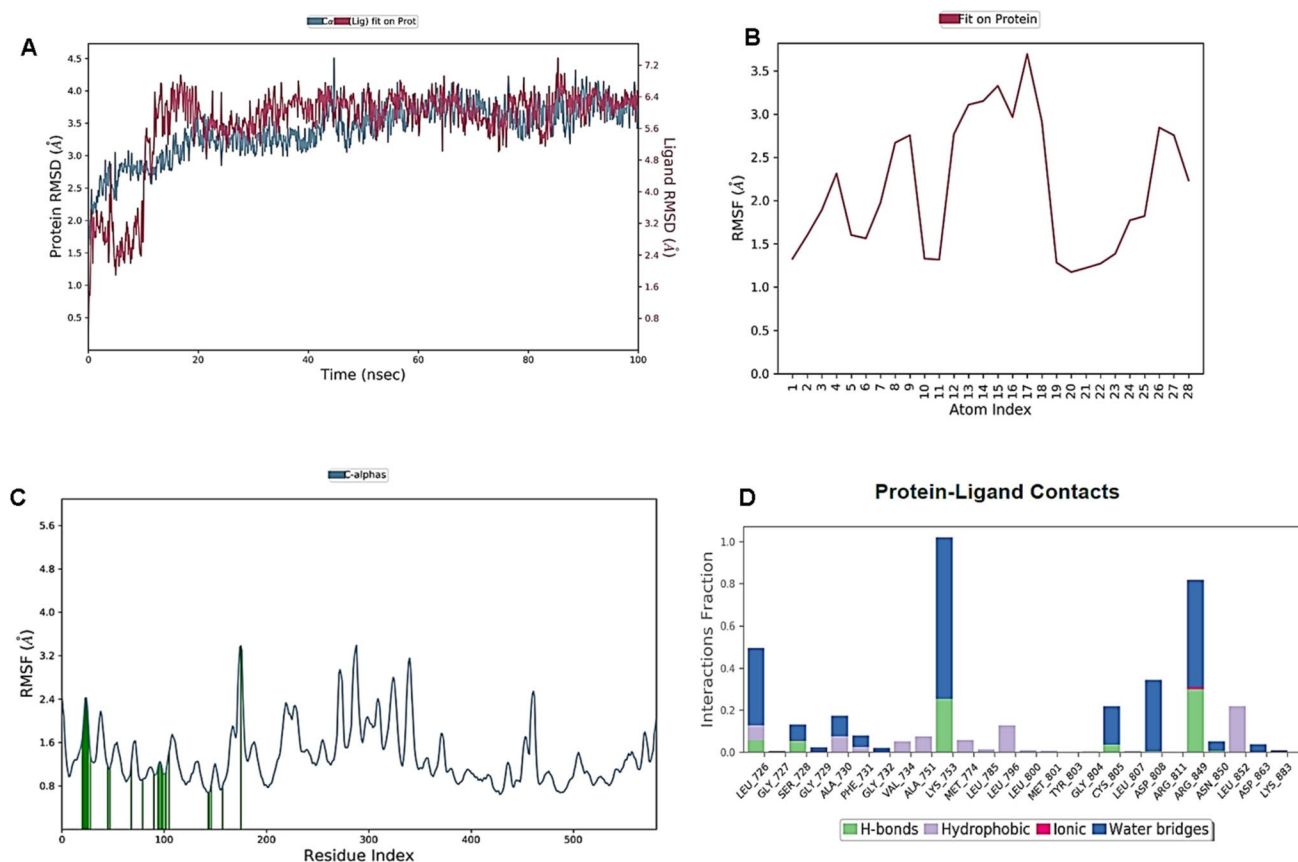


**Fig. 5** **A** RMSD evolutions of docked complexes between the C-alpha atoms of HER2 protein and ligands in 100 ns simulation. **B** Residue wise Root Mean Square Fluctuations (RMSF) graph between HER2 protein and ligand in 100 ns simulation: RMSF plot obtained

from Ligand RMSF values. **C** RMSF plot obtained from protein RMSF values. **D** Protein-Ligand Contacts between HER2 cancer receptor protein and ligand compound in 100 ns simulation

hydrophobic interactions are most important in MD simulations to determine ligand–proteins complex and their findings represents that Thr and Ser (Threonine and Serine) are the most significant residues in terms of H-bonds (Rasheed et al. 2021).

## 4 Conclusion

The conclusive findings shows that bioactive metabolite extracted from soil derived *Bacillus subtilis* was cytotoxic to human breast cancer MCF-7 and after in silico studies support these results as the bioactive metabolite showed promising binding energy of  $-8.8$  kcal/mol against HER2. The dynamic simulation results of this HER2 docked complex shows that HER2 have stable interaction towards ligand, hence it was predicted that bioactive ligand compound can interact with human HER2 cancer protein and can be used as anti-cancer compound to treat breast cancer.

**Authors contribution** Ayesha Irfan Hashmi (AIH); investigations, data curation, data analysis, wrote first draft, Mehwish Iqtedar (MI); conceptualization, supervision, resources, project administration, manuscript editing and review, Hamid Saeed (HS); resources, data analysis, validation, manuscript editing and review, Nadeem Ahmed (NA); data curation, data analysis, validation, Roheena Abdullah (RA); data curation, investigation, manuscript editing and review, Afshan Kaleem (AK); investigations, software, data analysis, visualization, Muhammad Athar Abbasi (MAA); Investigations, data analysis, validation.

**Funding** None.

**Data availability** Will be available on reasonable request to the corresponding authors.

## Declarations

**Competing interests** The authors have no relevant financial or non-financial interests to disclose.

**Ethics declaration** Not applicable.

**Open Access** This article is licensed under a Creative Commons Attribution-NonCommercial-NoDerivatives 4.0 International License, which permits any non-commercial use, sharing, distribution and reproduction in any medium or format, as long as you give appropriate credit to the original author(s) and the source, provide a link to the Creative Commons licence, and indicate if you modified the licensed material. You do not have permission under this licence to share adapted material derived from this article or parts of it. The images or other third party material in this article are included in the article's Creative Commons licence, unless indicated otherwise in a credit line to the material. If material is not included in the article's Creative Commons licence and your intended use is not permitted by statutory regulation or exceeds the permitted use, you will need to obtain permission directly from the copyright holder. To view a copy of this licence, visit <http://creativecommons.org/licenses/by-nc-nd/4.0/>.

## References

- Abdelaziz AA, Kamer AMA, Al-Monofy KB, Al-Madboly LA (2022) A purified and lyophilized *Pseudomonas aeruginosa* derived pyocyanin induces promising apoptotic and necrotic activities against MCF-7 human breast adenocarcinoma. *Microb Cell Fact* 21(1):262. <https://doi.org/10.1186/s12934-022-01988-x>
- Abdel-Nasser A, Badr AN, Fathy HM, Ghareeb MA, Barakat OS, Hathout AS (2024) Antifungal, antiaflatoxicogenic, and cytotoxic properties of bioactive secondary metabolites derived from *Bacillus* species. *Sci Rep* 14(1):16590. <https://doi.org/10.1038/s41598-024-66700-y>
- Abdulkadir M, Waliyu S (2012) Screening and isolation of soil bacteria for their ability to produce antibiotics. *Eur J Appl Sci* 4(5):211. <https://doi.org/10.5829/idosi.ejas.2012.4.5.2011>
- Aganja RP, Sivasankar C, Senevirathne A, Lee JH (2022) Salmonella as a promising curative tool against cancer. *Pharmaceutics* 14(10):2100. <https://doi.org/10.3390/pharmaceutics14102100>
- Agour MA, Hamed AA, Ghareeb MA, Abdel-Hamid EA, Ibrahim MK (2022) Bioactive secondary metabolites from marine *Actinomyces* sp. AW6 with an evaluation of ADME-related physicochemical properties. *Arch Microbiol* 204(8):537. <https://doi.org/10.1007/s00203-022-03092-5>
- Aimaier R, Li H, Cao W, Cao X, Zhang H, You J, Zhao H (2023) The secondary metabolites of *Bacillus subtilis* strain Z15 induce apoptosis in hepatocellular carcinoma cells. *Probiot Antimicrob Proteins* 31:1–11. <https://doi.org/10.1007/s12602-023-10181-4>
- Akbari A, Razzaghi Z, Homaei F, Khayamzadeh M, Movahedi M, Akbari ME (2011) Parity and breastfeeding are preventive measures against breast cancer in Iranian women. *Breast Cancer* 18:51–55. <https://doi.org/10.1007/s12282-010-0203-z>
- Akbarizare M, Ofoghi H, Hadizadeh M, Moazami N (2020) In vitro assessment of the cytotoxic effects of secondary metabolites from *Spirulina platensis* on hepatocellular carcinoma. *Egypt Liver J* 10:1–8. <https://doi.org/10.1186/s43066-020-0018-3>
- Alanazi AS, Mirgany TO, Alsouk AA, Alsaif NA, Alanazi MM (2023) Antiproliferative activity, multikinase inhibition, apoptosis-inducing effects and molecular docking of novel isatin-purine hybrids. *Medicina* 59(3):610. <https://doi.org/10.3390/medicina59030610>
- Ali HM, El-Shikh MS, Salem MZ (2016) Isolation of bioactive phenazine-1-carboxamide from the soil bacterium *Pantoea agglomerans* and study of its anticancer potency on different cancer cell lines. *J AOAC Int* 99(5):1233–1239. <https://doi.org/10.5740/jaoacint.16-0090>
- Anantha PS, Deventhiran M, Saravanan P, Anand D, Rajarajan S (2016) A comparative GC-MS analysis of bacterial secondary metabolites of *Pseudomonas* species. *Pharma Innov J* 5(4):84–89
- Arnold M, Morgan E, Rungay H, Mafra A, Singh D, Laversanne M, Soerjomataram I (2022) Current and future burden of breast cancer: global statistics for 2020 and 2040. *Breast* 66:15–23. <https://doi.org/10.1016/j.breast.2022.08.010>
- Ashfaq M, Afzal A, Javed MA, Ali M, Rasool B, Shaheen S, Rasheed A (2021) Identification and pathogenic characterization of bacteria causing rice grain discoloration in Pakistan. *Int J Biol Biotechnol* 18:239–346
- Ayan C, Uttam KR, Dinesh H (2017) Protein active site structure prediction strategy and algorithm. *Int J Curr Eng Technol* 7:1092–1096. <https://doi.org/10.14741/ijcet/22774106/7.3.2017.53>
- Ayuningrum D, Liu Y, Riyanti, Sibero MT, Kristiana R, Asagabaldan MA, Schaeberle TF (2019) Tunicate-associated bacteria show a great potential for the discovery of antimicrobial compounds. *PLoS One* 14(3):e0213797. <https://doi.org/10.1371/journal.pone.0213797>



- Azizah MR, Hanum HA, Norahmawati E, Fakurazi S, Kawamoto Y, Permana S, Endharti AT (2024) Systematic review on the efficacy and safety of ixabepilone-based chemotherapy regimen in triple-negative breast cancer. *J Pharm Pharmacogn Res* 12(4):722–734. [https://doi.org/10.56499/jppres23.1869\\_12.4.722](https://doi.org/10.56499/jppres23.1869_12.4.722)
- Balogun TA, Iqbal MN, Saibu OA, Akintubosun MO, Lateef OM, Nneka UC, Omoboyowa DA (2022) Discovery of potential HER2 inhibitors from *Mangifera indica* for the treatment of HER2-positive breast cancer: an integrated computational approach. *J Biomol Struct Dyn* 40(23):12772–12784. <https://doi.org/10.1080/07391102.2021.1975570>
- Behzadi R, Hormati A, Eivaziatashbeik K, Ahmadpour S, Khodadust F, Zaboli F, Seidi K (2021) Evaluation of anti-tumor potential of *Lactobacillus acidophilus* ATCC4356 culture supernatants in MCF-7 breast cancer. *Anti-Cancer Agents Med Chem* 21(14):1861–1870. <https://doi.org/10.2174/1871520621666201207085239>
- Bellemain E, Carlsen T, Brochmann C, Coissac E, Taberlet P, Kausarud H (2010) ITS as an environmental DNA barcode for fungi: an in silico approach reveals potential PCR biases. *BMC Microbiol* 10:1–9. <https://doi.org/10.1186/1471-2180-10-189>
- Burianek LL, Yousef AE (2000) Solvent extraction of bacteriocins from liquid cultures. *Lett Appl Microbiol* 31(3):193–197. <https://doi.org/10.1046/j.1365-2672.2000.00802.x>
- Burke MJ, Ziegler DS, Bautista F, Attarbaschi A, Gore L, Locatelli F, Baruchel A (2022) Phase 1b study of carfilzomib with induction chemotherapy in pediatric relapsed/refractory acute lymphoblastic leukemia. *Pediatr Blood Cancer* 69(12):e29999. <https://doi.org/10.1002/pbc.29999>
- Burley SK, Bhikadiya C, Bi C, Bittrich S, Chen L, Crichlow GV et al (2021) RCSB Protein Data Bank: powerful new tools for exploring 3D structures of biological macromolecules for basic and applied research and education in fundamental biology, biomedicine, biotechnology, bioengineering, and energy sciences. *Nucleic Acids Res* 49:D437–D451. <https://doi.org/10.1093/nar/gkaa1038>
- Caicedo NH, Kumirska J, Neumann J, Stolte S, Thöming J (2012) Detection of bioactive exometabolites produced by the filamentous marine cyanobacterium *Geitlerinema* sp. *Mar Biotechnol* 14:436–445. <https://doi.org/10.1007/s10126-011-9424-1>
- Carradori S, Guglielmi P, Luisi G, Secci D (2022) Nitrogen- and sulfur-containing heterocycles as dual antioxidant and anticancer agents. In *Handbook of oxidative stress in cancer: Mechanistic Aspects*. Springer Nature Singapore, pp. 2571–2588. [https://doi.org/10.1007/978-981-15-9411-3\\_180](https://doi.org/10.1007/978-981-15-9411-3_180)
- Caulier S, Nannan C, Gillis A, Licciardi F, Bragard C, Mahillon J (2019) Overview of the antimicrobial compounds produced by members of the *Bacillus subtilis* group. *Front Microbiol* 10:302. <https://doi.org/10.3389/fmicb.2019.00302>
- Chalasani AG, Dhanarajan G, Nema S, Sen R, Roy U (2015) An antimicrobial metabolite from *Bacillus* sp: significant activity against pathogenic bacteria including multidrug-resistant clinical strains. *Front Microbiol* 6:1335. <https://doi.org/10.3389/fmicb.2015.01335>
- Chen H, Cui J, Wang P, Wang X, Wen J (2020) Enhancement of bleomycin production in *Streptomyces verticillus* through global metabolic regulation of N-acetylglucosamine and assisted metabolic profiling analysis. *Microb Cell Fact* 19:1–17. <https://doi.org/10.1186/s12934-020-01301-8>
- Cousins KR (2011) Computer review of ChemDraw Ultra 12.0. *J Am Chem Soc* 133(21):8388. <https://doi.org/10.1021/ja204075s>
- Cristofanilli M (2012) Advancements in the treatment of metastatic breast cancer (MBC): the role of ixabepilone. *J Oncol* 2012(1):703858. <https://doi.org/10.1155/2012/703858>
- Daina A, Michielin O, Zoete V (2017) SwissADME: a free web tool to evaluate pharmacokinetics, drug-likeness, and medicinal chemistry friendliness of small molecules. *Sci Rep* 7:42717. <https://doi.org/10.1038/srep42717>
- Dan AK, Manna A, Ghosh S, Sikdar S, Sahu R, Parhi PK, Parida S (2021) Molecular mechanisms of the lipopeptides from *Bacillus subtilis* in the apoptosis of cancer cells - a review on its current status in different cancer cell lines. *Adv Cancer Biol Metastasis* 3:10001. <https://doi.org/10.1016/j.adcanc.2021.100019>
- Drakontaeidi A, Papanotas I, Pontiki E (2024) Multitarget pharmacology of sulfur–nitrogen heterocycles: anticancer and antioxidant perspectives. *Antioxidants* 13(8):898. <https://doi.org/10.3390/antiox13080898>
- Elmanama IA, Elmanama AA, Al Zaharna MM, Al-Reefi MR (2020) In vitro anticancer activity effect of extracellular metabolites of some bacterial species on HeLa cell line. *IUG J Nat Stud* 28(2). <https://doi.org/10.33976/IUGNS.28.2/2020/2>
- En-Nahli F, Baammi S, Hajji H, Alaqrabeh M, Lakhliifi T, Bouachrine M (2023) High-throughput virtual screening approach of natural compounds as target inhibitors of plasmepsin-II. *J Biomol Struct Dyn* 41(19):10070–10080. <https://doi.org/10.1080/07391102.2022.2152871>
- Faruk M (2021) Breast cancer resistance to chemotherapy: When should we suspect it and how can we prevent it? *Ann Med Surg* 70:102793. <https://doi.org/10.1016/j.amsu.2021.102793>
- Franzoi MA, Agostinetti E, Perachino M, Del Mastro L, de Azambuja E, Vaz-Luis I, Lambertini M (2021) Evidence-based approaches for the management of side-effects of adjuvant endocrine therapy in patients with breast cancer. *Lancet Oncol* 22(7):e303–e313. [https://doi.org/10.1016/S1470-2045\(20\)30666-5](https://doi.org/10.1016/S1470-2045(20)30666-5)
- Gam LH (2012) Breast cancer and protein biomarkers. *World J Exp Med* 2(5):86–91. <https://doi.org/10.5493/wjem.v2.i5.86>
- Gay F, Günther A, Offidani M, Engelhardt M, Salvini M, Montefusco V, Gramatzki M (2021) Carfilzomib, bendamustine, and dexamethasone in patients with advanced multiple myeloma: the EMN09 phase 1/2 study of the European myeloma network. *Cancer* 127(18):3413–3421. <https://doi.org/10.1002/cncr.33647>
- Gil-Turnes MS, Hay ME, Fenical W (1989) Symbiotic marine bacteria chemically defend crustacean embryos from a pathogenic fungus. *Science* 246(4926):116–118. <https://doi.org/10.1126/science.2781297>
- Gislind D, Sudarsanam D, Raj GA, Baskar K (2018) Antibacterial activity of soil bacteria isolated from Kochi, India and their molecular identification. *J Genet Eng Biotechnol* 16(2):287–294. <https://doi.org/10.1016/j.jgeb.2018.05.010>
- Grafe U, Radics L (1986) Isolation and structure elucidation of 6-(3'-methylbuten-2'-yl) isatin, an unusual metabolite from *Streptomyces albus*. *J Antibiot* 39(1):162–163. <https://doi.org/10.7164/antibiotics.39.162>
- Hamed AA, Ghada Abdel-Razik G, Battah MG, Hassan M (2024) Bioactive metabolites from *Streptomyces* sp RSE with potential anticancer and antioxidant activity. *Egypt J Chem* 67(4):115–125. <https://doi.org/10.21608/ejchem.2023.226993.8357>
- Houghton SC, Hankinson SE (2021) Cancer progress and priorities: breast cancer. *Cancer Epidemiol Biomarkers Prev* 30(5):822–844. <https://doi.org/10.1158/1055-9965.EPI-20-1193>
- Huang B, Kong L, Wang C, Ju F, Zhang Q, Zhu J, Gong T, Zhang H, Yu C, Zheng WM, Bu D (2023) Protein structure prediction: challenges, advances, and the shift of research paradigms. *Genomics Proteomics Bioinform* 21(5):913–925. <https://doi.org/10.1016/j.gpb.2022.11.014>
- Jeong SY, Ishida K, Ito Y, Okada S, Murakami M (2003) Bacillamide, a novel algicide from the marine bacterium, *Bacillus* sp. SY-1, against the harmful dinoflagellate *Cochlodinium polykrikoides*. *Tetrahedron Lett* 44(43):8005–8007. <https://doi.org/10.1016/j.tetlet.2003.08.115>

- Jeong SY, Park SY, Kim YH, Kim M, Lee SJ (2008) Cytotoxicity and apoptosis induction of *Bacillus vallismortis* BIT-33 metabolites on colon cancer carcinoma cells. *J Appl Microbiol* 104(3):796–807. <https://doi.org/10.1111/j.1365-2672.2007.03615.x>
- Kalia VC, Patel SK, Cho BK, Wood TK, Lee JK (2022) Emerging applications of bacteria as antitumor agents. *Semin Cancer Biol* 86:1014–1025. <https://doi.org/10.1016/j.semcancer.2021.05.012>
- Kannan MN, Sethi S, Badoni A, Chamoli V, Bahuguna NC (2018) Isolation and characterization of bacterial isolates from agriculture field soil of Roorkee region. *J Pharmacogn Phytochem* 7(5S):108–110
- Kaspar F, Neubauer P, Gimpel M (2019) Bioactive secondary metabolites from *Bacillus subtilis*: a comprehensive review. *J Nat Prod* 82(7):2038–2053. <https://doi.org/10.1021/acs.jnatprod.9b00110>
- Kennedy RK, Naik PR, Veena V, Lakshmi BS, Lakshmi P, Krishna R, Sakthivel N (2015) 5-Methyl phenazine-1-carboxylic acid: a novel bioactive metabolite by a rhizosphere soil bacterium that exhibits potent antimicrobial and anticancer activities. *Chem-Biol Interact*. <https://doi.org/10.1016/j.cbi.2015.03.002>
- Kumari NP, Ram MR (2021) Isolation and characterization of anticancerous bioactive compounds from marine *Bacillus subtilis*. *J Adv Sci Res* 12(02):203–211. <https://doi.org/10.55218/JASR.s2202112228>
- Kyrgiou M, Salanti G, Pavlidis N, Paraskevaidis E, Ioannidis JP (2006) Survival benefits with diverse chemotherapy regimens for ovarian cancer: meta-analysis of multiple treatments. *J Natl Cancer Inst* 98(22):1655–1663. <https://doi.org/10.1093/jnci/djj443>
- Laliani G, Sorboni SG, Lari R, Yaghoubi A, Soleimanpour S, Khazaei M, Avan A (2020) Bacteria and cancer: Different sides of the same coin. *Life Sci* 246:117398. <https://doi.org/10.1016/j.lfs.2020.117398>
- Laursen JB, Nielsen J (2004) Phenazine natural products: biosynthesis, synthetic analogues, and biological activity. *Chem Rev* 104(3):1663–1686. <https://doi.org/10.1021/cr020473j>
- Li J, Ren J, Sun W (2017) Systematic review of ixabepilone for treating metastatic breast cancer. *Breast Cancer* 24:171–179. <https://doi.org/10.1007/s12282-016-0717-0>
- Liu M, Jia Y, Xie Y, Zhang C, Ma J, Sun C, Ju J (2019) Identification of the actinomycin D biosynthetic pathway from marine-derived *Streptomyces costaricanus* SCSIO ZS0073. *Mar Drugs* 17(4):240. <https://doi.org/10.3390/md17040240>
- Liu Y, Lau HCH, Yu J (2023) Microbial metabolites in colorectal tumorigenesis and cancer therapy. *Gut Microbes* 15(1):2203968. <https://doi.org/10.1080/19490976.2023.2203968>
- Marcelo P, Gontier E, Dauwe R (2019) Metabolic markers for the yield of lipophilic indole alkaloids in dried woad leaves (*Isatis tinctoria* L.). *Phytochemistry* 163:89–98. <https://doi.org/10.1016/j.phytochem.2019.04.006>
- McCoy CS, Mannion AJ, Feng Y, Madden CM, Artim SC, Au GG, Fox JG (2021) Cytotoxic *Escherichia coli* strains encoding colibactin, cytotoxic necrotizing factor, and cytolethal distending toxin colonize laboratory common marmosets (*Callithrix jacchus*). *Sci Rep* 11(1):2309. <https://doi.org/10.1038/s41598-020-80000-1>
- Mishra APSS (2013) Isolation and biochemical characterization of antibiotic-producing microorganism from waste soil samples of certain industrial areas of India. <https://doi.org/10.9790/3008-0568089>
- Mitri Z, Constantine T, O'Regan R (2012) The HER2 receptor in breast cancer: pathophysiology, clinical use, and new advances in therapy. *Chemother Res Pract* 2012(1):743193. <https://doi.org/10.1155/2012/743193>
- Mohan CD, Rangappa S, Nayak SC, Jadimurthy R, Wang L, Sethi G, Rangappa KS (2022) Bacteria as a treasure house of secondary metabolites with anticancer potential. *Semin Cancer Biol* 86:998–1013. <https://doi.org/10.1016/j.semcancer.2021.05.006>
- Mosmann T (1983) Rapid colorimetric assay for cellular growth and survival: application to proliferation and cytotoxicity assays. *J Immunol Methods* 65(1–2):55–63. [https://doi.org/10.1016/0022-1759\(83\)90303-4](https://doi.org/10.1016/0022-1759(83)90303-4)
- Nakkarach A, Foo HL, Song AAL, Mutalib NEA, Nitisinprasert S, Withayagiat U (2021) Anti-cancer and anti-inflammatory effects elicited by short chain fatty acids produced by *Escherichia coli* isolated from healthy human gut microbiota. *Microb Cell Fact* 20:1–17. <https://doi.org/10.1186/s12934-020-01477-z>
- Nascimento Chaves KR, França MLT, Mendes ALO, Cardoso PP, Vasconcelos KBP, Santana RCF, Silva SKR (2024) Antibacterial, antioxidant and anticancer activities of the *Streptomyces* PML5 strain isolated from carbonate rocks in the Amazon. <https://doi.org/10.21203/rs.3.rs-4069286/v1>
- Numan M, Shah M, Asaf S, Ur Rehman N, Al-Harrasi A (2022) Bioactive compounds from endophytic bacteria *Bacillus subtilis* strain EP1 with their antibacterial activities. *Metabolites* 12(12):1228. <https://doi.org/10.3390/metabo12121228>
- Ongena M, Jacques P (2008) *Bacillus* lipopeptides: versatile weapons for plant disease biocontrol. *Trends Microbiol* 16(3):115–125. <https://doi.org/10.1016/j.tim.2007.12.009>
- Osama N, Bakeer W, Raslan M, Soliman HA, Abdelmohsen UR, Sebak M (2022) Anti-cancer and antimicrobial potential of five soil *Streptomyces*: A metabolomics-based study. *R Soc Open Sci* 9(2):211509. <https://doi.org/10.1098/rsos.211509>
- Partridge AH, Winer EP (2004) Long-term complications of adjuvant chemotherapy for early-stage breast cancer. *Breast Dis* 21(1):55–64. <https://doi.org/10.3233/BD-2004-21108>
- Pereira DM, Valentão P, Pereira JA, Andrade PB (2009) Phenolics: from chemistry to biology. *Molecules* 14(6):2202–2211. <https://doi.org/10.3390/molecules14062202>
- Raghava Rao KV, Mani P, Satyanarayana B, Raghava Rao T (2017) Purification and structural elucidation of three bioactive compounds isolated from *Streptomyces coelicoflavus* BC 01 and their biological activity. *Biotech* 7:1–12. <https://doi.org/10.1007/s13205-016-0581-9>
- Rahman H, Khan I, Hussain A, Shahat AA, Tawab A, Qasim M, Khan SN (2018) Glycyrrhiza glabra HPLC fractions: identification of Aldehydoisopropylpogonone and Liquiritigenin having activity against multidrug resistant bacteria. *BMC Complement Altern Med* 18:1–6. <https://doi.org/10.1186/s12906-018-2207-8>
- Rajivgandhi G, Muneeswaran T, Maruthupandy M, Ramakritinan CM, Saravanan K, Ravikumar V, Manoharan N (2018) Antibacterial and anticancer potential of marine endophytic actinomycetes *Streptomyces coeruleorubidus* GRG 4 (KY457708) compound against colistin-resistant uropathogens and A549 lung cancer cells. *Microb Pathog* 125:325–335. <https://doi.org/10.1016/j.micpath.2018.09.025>
- Rasheed MA, Iqbal MN, Saddick S, Ali I, Khan FS, Kanwal S, Awais M (2021) Identification of lead compounds against *Scm* (fms10) in *Enterococcus faecium* using computer-aided drug designing. *Life* 11(2):77. <https://doi.org/10.3390/life11020077>
- Riaz A, Kaleem A, Abdullah R, Iqtedar M, Hoessli DC, Aftab M (2024) In silico approaches to study the human asparagine synthetase: An insight of the interaction between the enzyme active sites and its substrates. *PLoS ONE* 19(8):e0307448. <https://doi.org/10.1371/journal.pone.0307448>
- Ritchie TJ, Ertl P, Lewis R (2011) The graphical representation of ADME-related molecule properties for medicinal chemists. *Drug Discov Today* 16(1–2):65–72. <https://doi.org/10.1016/j.drudis.2010.11.002>
- Sait KHW, Mashrafi M, Khogeer AA, Alzahrani O, Anfinan NM, Sait HK, Almutairi A, Alam Q (2020) Molecular docking analysis of HER-2 inhibitor from the ZINC database as anticancer agents. *Bioinformation* 16(11):882–887. <https://doi.org/10.6026/97320630016882>

- Salazar B, Ortiz A, Keswani C, Minkina T, Mandzhieva S, Pratap Singh S, Sansinenea E (2023) *Bacillus* spp. as bio-factories for antifungal secondary metabolites: innovation beyond whole organism formulations. *Microb Ecol* 86(1):1–24. <https://doi.org/10.1007/s00248-022-02044-2>
- San-Diego CA (2021) USA, BIOVIA; Dassault Systèmes. Discovery Studio Visualizer. Dassault Systèmes, v21.1.0.20298.
- Schettini F, Pascual T, Conte B, Chic N, Brasó-Maristany F, Galván P, Prat A (2020) HER2-enriched subtype and pathological complete response in HER2-positive breast cancer: a systematic review and meta-analysis. *Cancer Treat Rev* 84:101965. <https://doi.org/10.1016/j.ctrv.2020.101965>
- Schrödinger L, DeLano W., 2020. PyMOL [Internet]. Available from: <http://www.pymol.org/pymol>
- Sebola TE, Uche-Okerefor NC, Mekuto L, Makatini MM, Green E (2020). Mavumengwana. <https://doi.org/10.1155/2020/8839490>
- Sereena MC, Sebastian D (2020) Evaluation of anticancer and anti-hemolytic activity of azurin, a novel bacterial protein from *Pseudomonas aeruginosa* SSj. *Int J Pept Res Ther* 26(1):459–466. <https://doi.org/10.1007/s10989-019-09851-1>
- Sethi Y, Vora V, Anyagwa OE, Turabi N, Abdelwahab M, Kaiwan O, Padda I (2024) *Streptomyces* paradigm in anticancer therapy: a state-of-the-art review. *Curr Cancer Ther Rev* 20(4):386–401. <https://doi.org/10.2174/0115733947254550230920170230>
- Shaaban KA, Shaaban M, Nair V, Schuhmann I, Win HY, Lei L, Laatsch H (2016) Structure elucidation and synthesis of hydroxylated isatins from *Streptomyces*. *Z Naturforsch B* 71(12):1191–1198. <https://doi.org/10.1515/znb-2016-0143>
- Shaikh S, Younis M, Yingying S, Tanziela T, Yuan L (2023) Bleomycin loaded exosomes enhanced antitumor therapeutic efficacy and reduced toxicity. *Life Sci* 330:121977. <https://doi.org/10.1016/j.lfs.2023.121977>
- Shalini TS, Manivel G, Ragothaman P, Velu RK, Senthilraja P (2024) Secondary metabolite profiling using HR-LCMS, antioxidant and anticancer activity of *Bacillus cereus* PSMS6 methanolic extract: In silico and in vitro study. *Biotechnol Rep* 42:e00842
- Shamsee ZR, Al-Saffar AZ, Al-Shanon AF, Al-Obaidi JR (2019) Cytotoxic and cell cycle arrest induction of pentacyclic triterpenoids separated from *Lantana camara* leaves against MCF-7 cell line in vitro. *Mol Biol Rep* 46:381–390. <https://doi.org/10.1007/s11033-018-4482-3>
- Shao Y, Wang XY, Qiu X, Niu LL, Ma ZL (2021) Isolation and purification of a new *Bacillus subtilis* strain from deer dung with antimicrobial and anti-cancer activities. *Curr Med Sci* 41:832–840. <https://doi.org/10.1007/s11596-021-2383-5>
- Sihem BM, Rafik E, Mathieu F, Mohamed C, Lebrihi A (2011) Identification and partial characterization of antifungal and antibacterial activities of two *Bacillus* sp. strains isolated from salt soil in Tunisia. *Afr J Microbiol Res* 5(13):1599. <https://doi.org/10.5897/AJMR11.073>
- Socha AM, Long RA, Rowley DC (2007) Bacillamides from a hypersaline microbial mat bacterium. *J Nat Prod* 70(11):1793–1795. <https://doi.org/10.1021/np070126a>
- Speranza J, Miceli N, Taviano MF, Ragusa S, Kwiecień I, Szopa A, Ekiert H (2020) *Isatis tinctoria* L. (Woad): A review of its botany, ethnobotanical uses, phytochemistry, biological activities, and biotechnological studies. *Plants* 9(3):298. <https://doi.org/10.3390/plants9030298>
- Subbiah U, Dinakarkumar Y, Jeyaraman M (2024) *Spongia officinalis*-associated *Pseudomonas fluorescens* as a reservoir of bioactive compounds: A novel source of natural anticancer compounds. *J Trop Biodivers Biotechnol* 9(3):90693. <https://doi.org/10.22146/jtbb.90693>
- Terefe EM, Ghosh A (2022) Molecular docking, validation, dynamics simulations, and pharmacokinetic prediction of phytochemicals isolated from *Croton dichogamus* against the HIV-1 reverse transcriptase. *Bioinform Biol Insights* 16:11779322221125604. <https://doi.org/10.1177/11779322221125604>
- Thomas AT, Rao JV, Subrahmanyam VM, Chandrashekhara HR, Maliyakkal N, Kisan TK, Joseph A, Udupa N (2011) In vitro anticancer activity of microbial isolates from diverse habitats. *Braz J Pharm Sci* 47(2):279–287. <https://doi.org/10.1590/S1984-82502011000200009>
- Thorn CF, Oshiro C, Marsh S, Hernandez-Boussard T, McLeod H, Klein TE, Altman RB (2011) Doxorubicin pathways: pharmacodynamics and adverse effects. *Pharmacogenet Genomics* 21(7):440–446. <https://doi.org/10.1097/FPC.0b013e32833fb566>
- Tran C, Cock IE, Chen X, Feng Y (2022) Antimicrobial *Bacillus*: metabolites and their mode of action. *Antibiotics* 11(1):88. <https://doi.org/10.3390/antibiotics11010088>
- Trayes KP, Cokenakes SE (2021) Breast cancer treatment. *Am Fam Phys* 104(2):171–178
- Triningsih DW, Harunari E, Fukaya K, Oku N, Urabe D, Igarashi Y (2023) Species-specific secondary metabolism by actinomycetes of the genus *Phytohabitans* and discovery of new pyranonaphthoquinones and isatin derivatives. *J Antibiot* 76(5):249–259. <https://doi.org/10.1038/s41429-023-00605-2>
- Trott O, Olson AJ (2010) AutoDock Vina: improving the speed and accuracy of docking with a new scoring function, efficient optimization, and multithreading. *J Comput Chem* 3:455–461. <https://doi.org/10.1002/jcc.21334>
- Tyc O, Song C, Dickschat JS, Vos M, Garbeva P (2017) The ecological role of volatile and soluble secondary metabolites produced by soil bacteria. *Trends Microbiol* 25(4):280–292. <https://doi.org/10.1016/j.tim.2016.12.002>
- Uddin MN, Chowdhury MH (2022) Enumeration, isolation, and characterization of bacteria of Gopalgur soil series of Bangladesh. *Interdiscip J Appl Basic Subj* 2(2):21–26. <https://doi.org/10.0002/ijabs-22b-06001>
- Wang Y, Wang Y, Sun T, Xu J (2024) Bacteriocins in cancer treatment: mechanisms and clinical potentials. *Biomolecules* 14(7):831. <https://doi.org/10.3390/biom14070831>
- White TJ, Bruns T, Lee SJWT, Taylor J (1990) Amplification and direct sequencing of fungal ribosomal RNA genes for phylogenetics. *PCR Protoc Guide Methods Appl* 18(1):315–322
- Wu C, Du C, Gubbens J, Choi YH, Van Wezel GP (2015) Metabolomics-driven discovery of a prenylated isatin antibiotic produced by *Streptomyces* species MBT28. *J Nat Prod* 78(10):2355–2363. <https://doi.org/10.1021/acs.jnatprod.5b00276>
- Yaghoubi A, Ghazvini K, Khazaei M, Hasanian SM, Avan A, Soleimanpour S (2022) The use of *Clostridium* in cancer therapy: a promising way. *Rev Res Med Microbiol* 33(2):121–127. <https://doi.org/10.1097/MRM.0000000000000281>
- Zhang KP, Fang X, Zhang Y, Chao M (2021) The prognosis of cancer patients undergoing liposomal doxorubicin-based chemotherapy: a systematic review and meta-analysis. *Medicine* 100(34):e26690. <https://doi.org/10.1097/MD.00000000000026690>
- Zhang S, Croppi G, Hu H, Li Y, Zhu C, Wu F, Li Z (2022) Bacillamide F, extracted from marine *Bacillus atrophaeus* C89, preliminary effects on leukemia cell lines. *Biology* 11(12):1712. <https://doi.org/10.3390/biology11121712>
- Zhang S, Jin Z, Bao L, Shu P (2024) The global burden of breast cancer in women from 1990 to 2030: assessment and projection based on the global burden of disease study 2019. *Front. Oncol* 14:1364397. <https://doi.org/10.3389/fonc.2024.1364397>